

Supporting Information

Hierarchical Mn-Ni₂P/NiFe LDH nanosheets arrays as an efficient bifunctional electrocatalyst for energy-saving hydrogen production *via* urea electrolysis

Bin Sang,^b Yu Liu,^a Xiaoyu Wan,^{a*} Shuixiang Xie,^a Guangyu Zhang,^a Mingzheng Ge,^a Jiamu Dai,^a Wei Zhang,^{a*} and Rui-Qing Li^{a*}

^a School of Textile and Clothing, Nantong University, Nantong 226019, China

^b School of Chemistry and Chemical Engineering, Liaocheng University, Liaocheng 252059, China

Corresponding author: liruiqing@ntu.edu.cn; 2022081@ntu.edu.cn;
zhangwei@ntu.edu.cn

1. Experimental

1.1. Chemicals reagents

$\text{Ni}(\text{NO}_3)_2 \cdot 6\text{H}_2\text{O}$, $\text{MnCl}_2 \cdot 4\text{H}_2\text{O}$, NH_4F , $\text{Fe}(\text{NO}_3)_3 \cdot 9\text{H}_2\text{O}$, urea and NaH_2PO_2 were obtained from Sinopharm Chemical Reagent Co. Ltd. KOH was obtained from Adamas-beta®. NF was obtained from Taiyuan source of power company.

1.2. Samples preparation

1.2.1 Preparation of Mn-Ni₂P

NF (3 cm × 1 cm) was ultrasonically treated for 30 min in HCl aqueous solution followed by subsequent washing of water and ethanol to eliminate impurities and oxides on the surface. The Mn-Ni₂P was synthesized through following process. Firstly, 1.9 mmol $\text{Ni}(\text{NO}_3)_2$, 0.1 mmol MnCl_2 , 6 mmol NH_4F and 10 mmol urea were mixed in 35 mL distilled water. Then, NF was added into above solution, which was heated at 120 °C for 6 h. After that, Mn-NiOH precursor was washed, and heated in air at 70 °C. Secondly, the Mn-NiOH was further baked to 320 °C for 2h in N₂ with 0.9g NaH_2PO_2 as P source to prepare the Mn-Ni₂P.

1.2.2 Preparation of the Mn-Ni₂P/NiFe LDH

Typically, 0.25 mmol $\text{Ni}(\text{NO}_3)_2$, 0.25 mmol $\text{Fe}(\text{NO}_3)_3$, 3 mmol NH_4F and 5 mmol urea were added in water with stirring to get a uniform solution. Then, the Mn-Ni₂P was submerged in above solution and shifted into 50 mL autoclave, which was maintained for 6 h at 120 °C. After that, the Mn-Ni₂P/NiFe LDH was prepared after washing and placed at 70 °C for 12 h.

1.3. Samples characterization

Phases and components of obtained products was recorded by powder X-ray diffraction (XRD, Bruker D8). The morphology was visualized by scanning electron microscopy (SEM, S-4800) and transmission electron microscopy (TEM, FEI Talos F200X). The surface formation and element valence of products was determined by X-ray photoelectron spectrometer (XPS, Thermo ESCALAB 250).

1.4. Electrochemical measurements

Electrochemical tests were implemented in standard three-electrode system by biologic VMP3 electrochemical workstation, and obtained materials was employed as working

electrodes. The catalytic behavior was measured at a scan rate of 2 mV s^{-1} in alkaline electrolyte without and with 0.5 M urea. All potentials were rectified. Electrocatalytic active area (ECSA) was tested at diverse scan rates in non-Faradaic region. Electrochemical impedance spectroscopy (EIS) was performed at a frequency from 100 kHz to 0.01 Hz with a 5 mV AC amplitude.

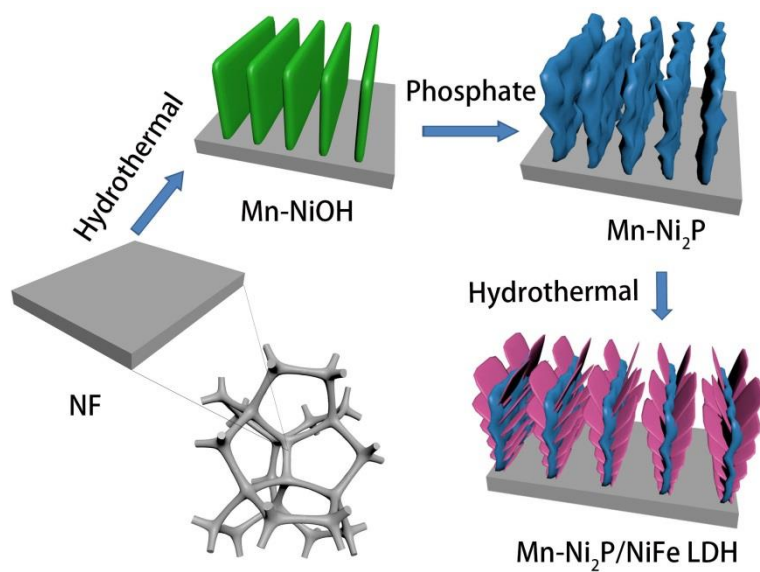


Fig. S1. Schematic diagram for synthesizing Mn-Ni₂P/NiFe LDH.

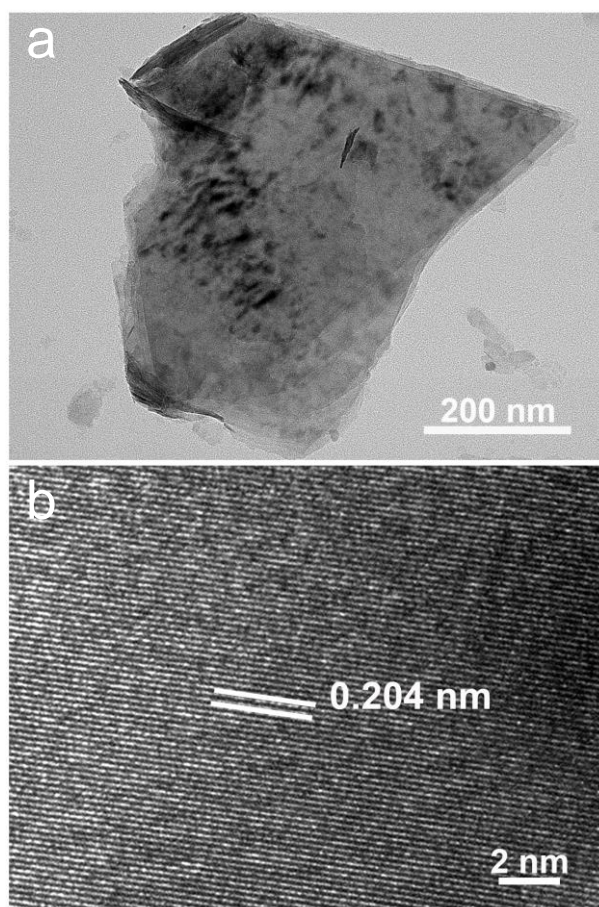


Fig. S2. (a) TEM and (b) HRTEM images of Mn-NiOH and Mn-Ni₂P.

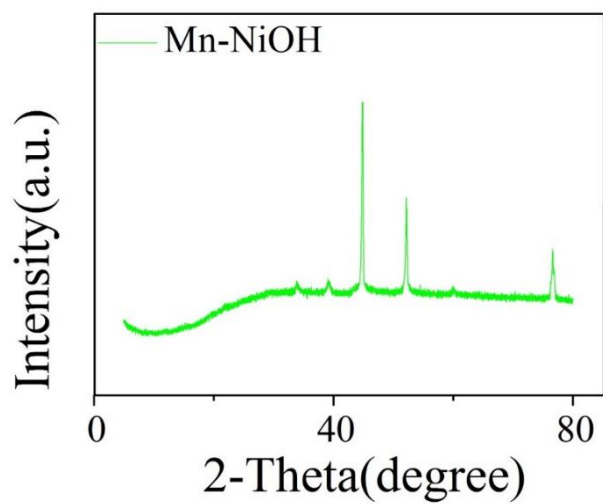


Fig. S3. XRD pattern of Mn-NiOH.

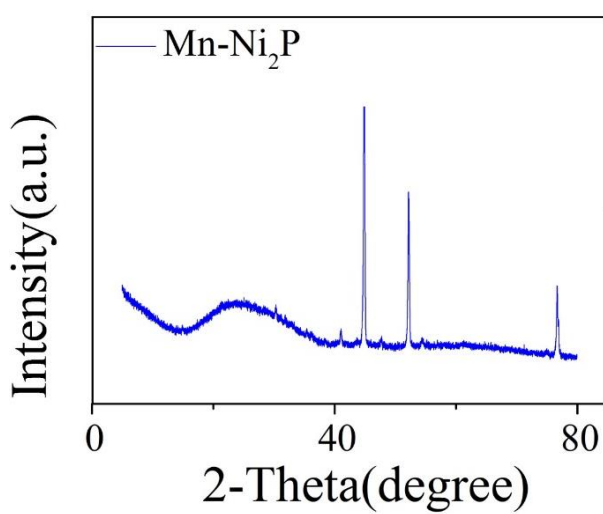


Fig. S4. XRD pattern of Mn-Ni₂P.

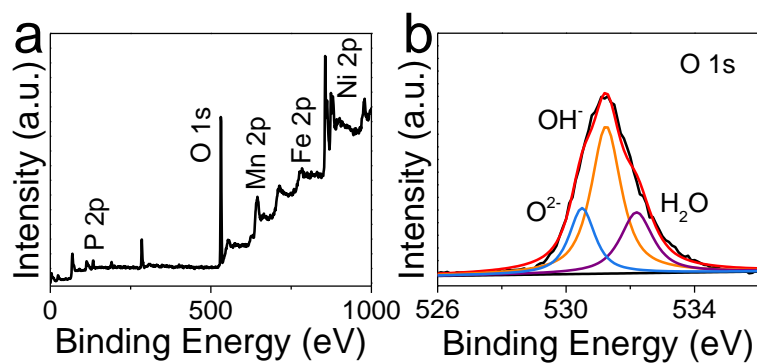


Fig. S5. XPS spectra of (a) survey scan and (b) O 1s for Mn-Ni₂P/NiFe LDH.

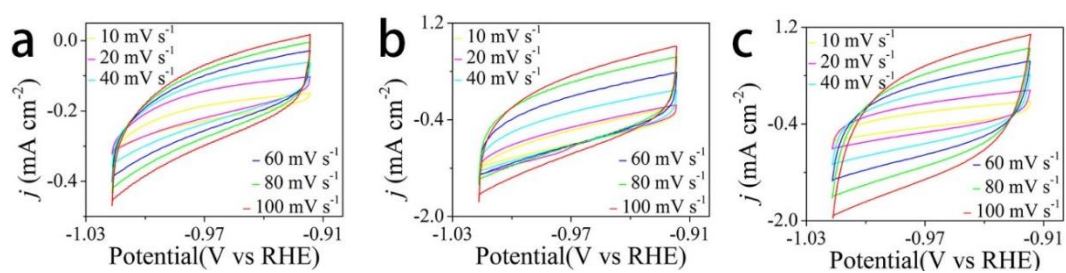


Fig. S6. CV curves of Ni₂P (a), Mn-Ni₂P (b), and Mn-Ni₂P/NiFe LDH (c).

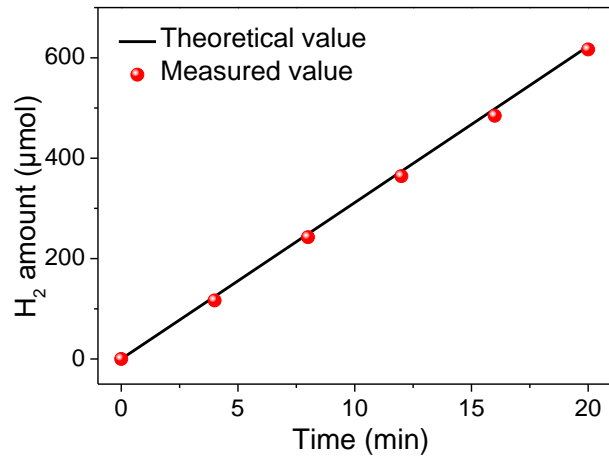


Fig. S7. Experimental and theoretical calculated amount of evolved H₂ over the Mn-Ni₂P/NiFe LDH.

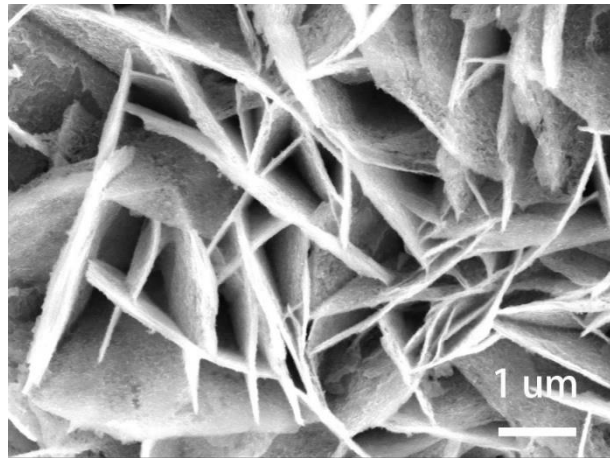


Fig. S8. SEM image of Mn-Ni₂P/NiFe LDH after HER stability.

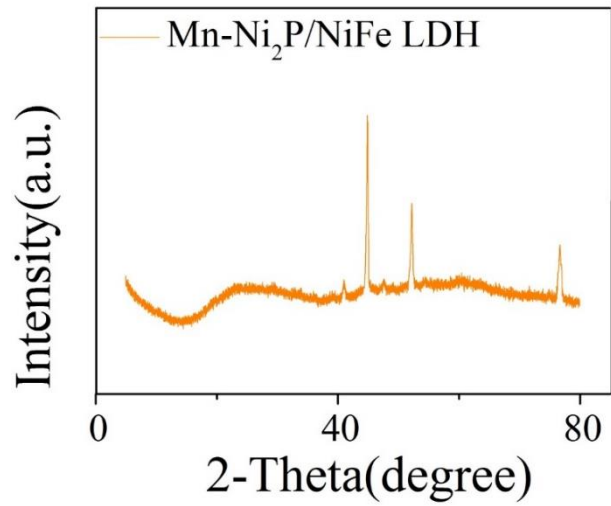


Fig. S9. XRD pattern of the Mn-Ni₂P/NiFe LDH after HER stability.

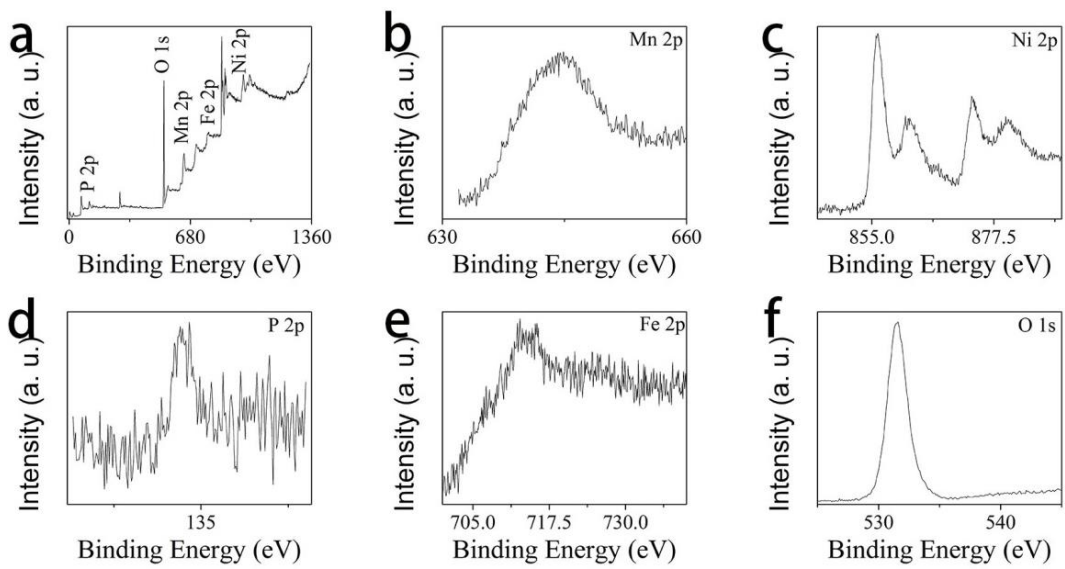


Fig. S10. XPS spectra of (a) survey scan, (b) Mn 2p, (c) Ni 2p, (d) P 2p, (e) Fe 2p and (f) O 1s for the Mn-Ni₂P/NiFe LDH after HER stability.

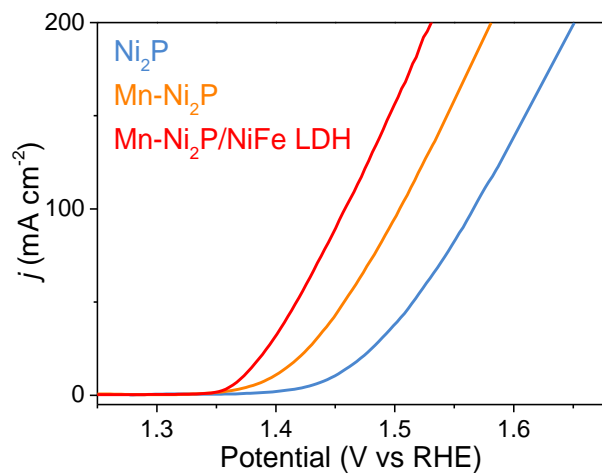


Fig. S11. LSV curves of Ni₂P, Mn-Ni₂P and Mn-Ni₂P/NiFe LDH in 1.0 M KOH with 0.5 M urea.

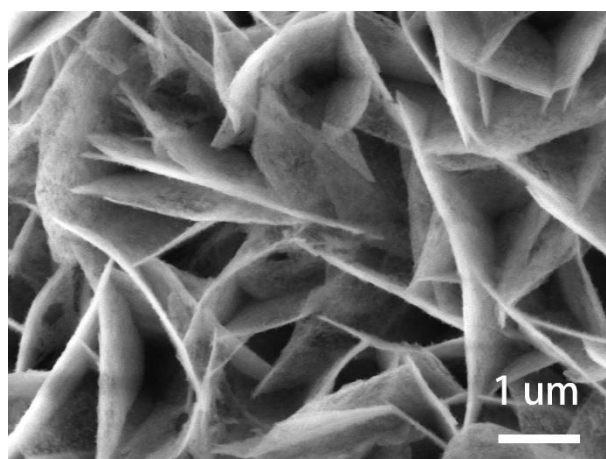


Fig. S12. SEM image of Mn-Ni₂P/NiFe LDH after UOR stability.

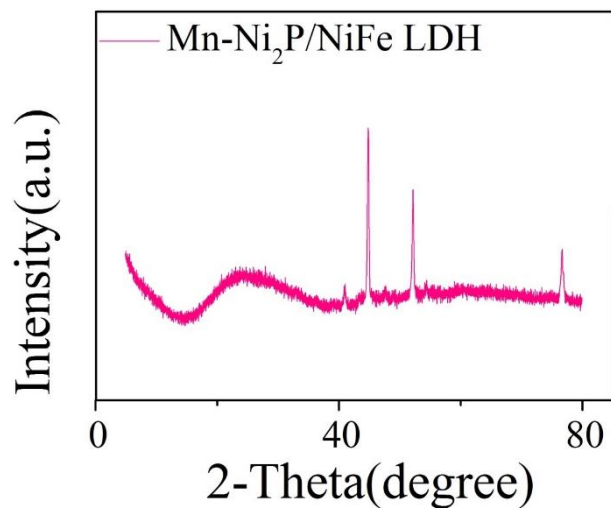


Fig. S13. XRD pattern of the Mn-Ni₂P/NiFe LDH after UOR stability.

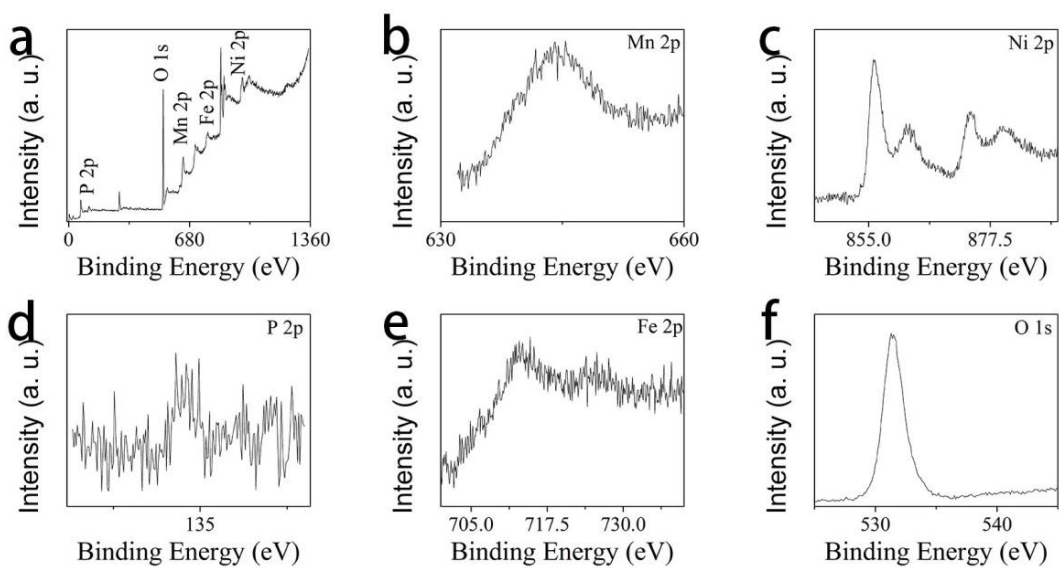


Fig. S14. XPS spectra of (a) survey scan, (b) Mn 2p, (c) Ni 2p, (d) P 2p, (e) Fe 2p and (f) O 1s for Mn-Ni₂P/NiFe LDH after UOR stability.

Table S1. Comparison of UOR performance of Mn-Ni₂P/NiFe LDH with other reported catalysts.

Catalysts	Overpotential (V) at 10 mA cm ⁻²	References
Mn-Ni₂P/NiFe LDH	1.372	This work
Fe ₃ O ₄ @FeOOH-NF	1.38	[S1]
Fe ₂ O ₃ /NF	1.41	[S1]
Ni/SiO _x /N-C	1.38	[S2]
NiMoSe	1.39	[S3]
Ce-Ni ₂ P/NF	1.4	[S4]
NiMo@ZnO/NF	1.4	[S5]
Fe-Ni ₃ S ₂ @FeNi ₃	1.4	[S6]
Ni ₂ P/NiF ₃ /CC	1.4	[S7]
Mo-Ni ₂ P	1.41	[S8]
Ni ₂ P/CFC	1.42	[S9]
P-CoS ₂	1.51	[S10]

Table S2. Comparison of water splitting performances of Mn-Ni₂P/NiFe LDH with recently reported catalysts.

Catalysts	Voltage (V) at 10 mA cm ⁻²	References
Mn-Ni₂P/NiFe LDH	1.632	This work
NiMo-PVP/NiFe-PVP	1.66	[S11]
Ni/Mo ₂ C-PC	1.66	[S12]
NiFe/NiCo ₂ O ₄ /Ni foam	1.67	[S13]
SrNb _{0.1} Co _{0.7} Fe _{0.2} O _{3-δ} perovskite	1.68	[S14]
Ni ₅ P ₄ /Ni foil	1.7	[S15]
Co _x P@NC	1.71	[S16]
Co ₂ B/CoSe ₂	1.73	[S17]
V/Ni foam	1.74	[S18]
CoPS/Al ₂ O ₃ -3	1.75	[S19]
Co/CeO ₂ /Co ₂ P/CoP@NC	1.76	[S20]

Table S3. Comparison of urea electrolysis performances of Mn-Ni₂P/NiFe LDH with recently reported catalysts.

Catalysts	Voltage (V) at 10 mA cm ⁻²	References
Mn-Ni₂P/NiFe LDH	1.494	This work
CoMn/CoMn ₂ O ₄	1.51	[S21]
NiTe ₂ /Ni(OH) ₂	1.52	[S22]
Ni-MOF	1.52	[S23]
Fe ₇ Se ₈ @Fe ₂ O ₃	1.55	[S24]
Bulk MnO ₂	1.55	[S25]
Ni@NCNT-3	1.56	[S26]
MnO ₂ /MnCo ₂ O ₄ /Ni	1.58	[S27]
FQD/CoNi LDH/NF	1.59	[S28]
HC-NiMoS/Ti	1.59	[S29]
Ni(OH) ₂ NS@NW/NF	1.68	[S30]

References

- [S1] H.A. Bandal, H. Kim, *J. Colloid Interf. Sci.*, 2022, **627**, 1030.
- [S2] M.J. Yuan, X.T. Guo, N. Li, H. Pang, *J. Colloid Interf. Sci.*, 2021, **589**, 56.
- [S3] H.T. Wang, X. Jiao, W.L. Zeng, Y. Zhang, Y.L. Jiao, *Int. J. Hydrogen Energ.*, 2021, **46**, 37792.
- [S4] K. Xiong, L.J. Yu, Y. Xiang, H.D. Zhang, J. Chen, Y. Gao, *J. Alloy. Compd.*, 2022, **912**, 165234.
- [S5] J. Cao, H.C. Li, R.T. Zhu, L. Ma, K.C. Zhou, Q.P. Wei, F.H. Luo, *J. Alloy. Compd.*, 2020, **844**, 155382.
- [S6] W.X. Zhang, Q. Jia, H. Liang, L. Cui, D. Wei, J.Q. Liu, *Chem. Eng. J.*, 2020, **396**, 125315.
- [S7] K.L. Wang, W. Huang, Q.H. Cao, Y.J. Zhao, X.J. Sun, R. Ding, W.W. Lin, E.H. Liu, P. Gao, *Chem. Eng. J.*, 2022, **427**, 130865.
- [S8] K. Zhang, G. Zhang, J.H. Qu, H.J. Liu, *J. Mater. Chem. A*, 2018, **6**, 10297.
- [S9] X. Zhang, Y.Y. Liu, Q.Z. Xiong, G.Q. Liu, C.J. Zhao, G.Z. Wang, Y.X. Zhang, H.M. Zhang, H.J. Zhao, *Electrochim. Acta.*, 2017, **254**, 44.
- [S10] Y. Jiang, S.S. Gao, J.L. Liu, G.C. Xu, Q. Jia, F.S. Chen, X.M. Song, *Nanoscale*, 2020, **12**,

11573.

[S11] Y.Q. Zhang, X.H. Xia, X. Cao, B.W. Zhang, N.H. Tiep, H.Y. He, S. Chen, Y.Z. Huang, H.J. Fan, *Adv. Energy Mater.*, 2017, **7**, 1700220.

[S12] Z.Y. Yu, Y. Duan, M.R. Gao, C.C. Lang, Y.R. Zheng, S.H. Yu, *Chem. Sci.*, 2017, **8**, 968.

[S13] C.L. Xiao, Y.B. Li, X.Y. Lu, C. Zhao, *Adv. Funct. Mater.*, 2016, **26**, 3515.

[S14] Y.L. Zhu, W. Zhou, Y.J. Zhong, Y.F. Bu, X.Y. Chen, Q. Zhong, M.L. Liu, Z.P. Shao, *Adv. Energy Mater.*, 2017, **7**, 1602122.

[S15] M. Ledendecker, S.K. Calderon, C. Papp, H.P. Steinruck, M. Antonietti, M. Shalom, *Angew. Chem. Int. Ed.*, 2015, **127**, 12538.

[S16] J.S. Li, L.X. Kong, Z.X. Wu, S. Zhang, X.Y. Yang, J.Q. Sha, G.D. Liu, *Carbon*, 2019, **145**, 694.

[S17] Y. Guo, Z. Yao, C. Shang, E. Wang, *ACS Appl. Mater. Interfaces*, 2017, **9**, 39312.

[S18] Y. Yu, P. Li, X.F. Wang, W.Y. Gao, Z.X. Shen, Y.N. Zhu, S.L. Yang, W.G. Song, K.J. Ding, *Nanoscale*, 2016, **8**, 10731.

[S19] T. Wang, Y. Zhang, Y. Wang, J. Zhou, L. Wu, Y. Sun, X. Xu, W. Hou, X. Zhou, Y. Du, W. Zhong, *ACS Sustainable Chem. Eng.*, 2018, **6**, 10087.

[S20] X.Z. Song, Q.F. Su, S.J. Li, G.C. Liu, N. Zhang, W.Y. Zhu, Z.H. Wang, Z. Tan, *Int. J. Hydrogen Energy*, 2020, **45**, 30559.

[S21] C. Wang, H.L. Lu, Z.Y. Mao, C.L. Yan, G.Z. Shen, X.F. Wang, *Adv. Funct. Mater.*, 2020, **30**, 2000556.

[S22] B. Xu, X.D. Yang, X.P. Liu, W.X. Song, Y.Q. Sun, Q.S. Liu, H.X. Yang, C.C. Li, *J. Power Sources*, 2020, **449**, 227585.

[S23] S.S. Zheng, Y. Zheng, H.G. Xue, H. Pang, *Chem. Eng. J.*, 2020, **395**, 125166.

[S24] J.X. Li, X.Q. Du, X.S. Zhang, Z.P. Wang, *Int. J. Hydrogen Energy*, 2022, **47**, 35203.

[S25] S. Chen, J.J. Duan, A. Vasileff, S.Z. Qiao, *Angew. Chem. Int. Edit.*, 2016, **55**, 3804.

[S26] Q. Zhang, F.M.D. Kazim, S.X. Ma, K.G. Qu, M. Li, Y.G. Wang, H. Hu, W.W. Cai, Z.H. Yang, *Appl. Catal. B-Environ.*, 2021, **280**, 119436.

[S27] C.L. Xiao, S. Li, X.Y. Zhang, D.R. MacFarlane, *J. Mater. Chem. A*, 2017, **5**, 7825.

[S28] Y.Q. Feng, X. Wang, J.F. Huang, P.P. Dong, J. Ji, J. Li, L.Y. Cao, L.L. Feng, P. Jin, C.R. Wang, *Chem. Eng. J.*, 2020, **390**, 124525.

[S29] X.X. Wang, J.M. Wang, X.P. Sun, S. Wei, L. Cui, W.R. Yang, J.Q. Liu, *Nano Res.*, 2018, **11**, 988.

[S30] Z.H. Yue, S.Y. Yao, Y.Z. Li, W.X. Zhu, W.T. Zhang, R. Wang, J. Wang, L.J. Huang, D.Y. Zhao, J.L. Wang, *Electrochim. Acta.*, 2018, **268**, 211.